Spectrochimica Acta. Vol. 38A, No. 2, pp. 141–148, 1982
Printed in Great Britain.

0584–8539/82/020141–08$03.00/0

Vibrational spectroscopy and normal coordinate analysis of μ halo hexahalodialuminates ions $Al_2X_7^-$ (X = Cl, Br, I) in some salts and in Friedel–Crafts solutions

ALAIN MANTEGHETTI and ANTOINE POTIER*
Laboratoire des Acides Minéraux, L.A. 79, Université des Sciences et Techniques du Languedoc,
Place E. Bataillon, 34060 Montpellier, Cédex France

(*Received* 16 *June* 1981)

Abstract—Infrared and Raman spectra are reported for $(Me_4N)Al_2Cl_7$, $(Et_4N)Al_2Cl_7$, KAl_2Br_7 and $CsAl_2I_7$ in the solid state at ordinary temperature. An assignment for practically all the vibrational modes is proposed for the three ions $Al_2Cl_7^-$, $Al_2Br_7^-$ and $Al_2I_7^-$. To elucidate the species occurring in the Friedel-Crafts liquids [the $Ar:2AlX_3:HX$ liquid mixture (X = Cl, Br)], the spectra of these solutions were also recorded. The quasi identity of the halogenide part of the spectra with the previous one leads to the unique formulation $ArH_2^+Al_2X_7^-$ for these solutions, in these cases the $Al_2X_7^-$ ion appears at a higher local symmetry of the AlX_3 groups than in the solid state. An approximate valence force field calculation confirms the assignments. It also shows the transferability of force constants for a X–AlX_3 model. Spectroscopic particularities are explained in terms of different coupling between bridged and terminal stretching modes.

INTRODUCTION

Fusion of aluminium or gallium trihalides with alkaline or ammonium and alkylammonium halides often yields $M^IX.2M^{III}X_3$ solid compounds. X-rays as well as vibrational spectroscopy show that they are $M^I[Al_2X_7]$ or $M^I[Ga_2X_7]$ salts. Their anions are also found in the $M^IX - M^{III}X_3$ melts. More recently, $Ga_2Cl_7^-$ has been recognized as the major anionic species in the alkylbenzene $2\,GaCl_3:HCl$ mixtures (Friedel-Crafts solutions).

In a previous paper, here referred to as [1], the $Ga_2Cl_7^-$ vibration spectra was carefully analysed as a basis for future studies. The purpose of the present paper is a general analysis of the three $Al_2X_7^-$ (X = Cl, Br, I) anions. Infrared and Raman spectra of several known and new compounds have been recorded. The assignments are made and correlated with the assistance of a general localized VFF.

Known and new compounds

Table 1 presents the known solid compounds. The $Al_2Cl_7^-$ and $Al_2I_7^-$ series appear quite incomplete.

On another hand, as far as we know the vibrational studies bear only on melts[1a–f] and bring no sufficient information. More particularly, equilibria between numerous ionic species such as AlX_4^-, $Al_2X_7^-$, $Al_3X_{10}^-$... give intricate spectra and lead to some incertainties in the $Al_2X_7^-$ assignments.

In the case of $Al_2Cl_7^-$, this situation leads us to synthesize the new compounds $Me_4N[Al_2Cl_7]$ and $Et_4N[Al_2Cl_7]$ where the cations are sufficiently large to stabilize the lattice. For $Al_2Br_7^-$ and $Al_2I_7^-$ we have chosen, respectively, KAl_2Br_7 and $CsAl_2I_7$, this last being the only known iodine compound identified[2].

Table 1. Presently known compounds and molten salts containing $Al_2X_7^-$ anions

$Al_2Cl_7^-$	Crystal	Te_4^{2+}, $Pd_2(C_6H_6)_2^{2+}$, Tl^+*
	Melts	Li^+, Na^+, K^+, Cs^+, Bu_4N^+
$Al_2Br_7^-$	Crystal	Li^+, Na^+, K^+, Rb^+, Cs^+, (NH_4^+)
	Melts	K^+
$Al_2I_7^-$	Melts	Cs^+
	Crystal	

*Not obtained in this work.

The study of these solids is complemented by the recording of the i.r. spectra of alkylbenzene: $2AlX_3:HX$ liquid mixtures[3] that are, as we will see later, the ionic salts $ArH^+Al_2X_7^-$. This has been made with: X = Cl, Br and Ar = toluene, xylene and mesitylene. These spectra appear needed, not only from a chemical point of view, but also because, in the deformation range, the normal modes of the anion might be mixed with crystal modes. Furthermore, this allowed an expansion of the low frequency range down to 50 cm^{-1}.

EXPERIMENTAL

Syntheses

Crystals. $AlCl_3$ purified Merck aluminium chloride, mixed with pure grade aluminium was carried out by an HCl flow and finally sublimated twice.

$AlBr_3$ and AlI_3 were obtained by direct reaction between pure grade aluminium and the halogen. Their high hygroscopicity required a high quality dry atmosphere.

KAl_2Br_7 and $CsAl_2I_7$ were obtained by a vacuum melting of the stoechiometric mixtures $MX:2AlX_3$. The reactions ended after long annealing (10–30 h).

$Me_4N[Al_2Cl_7]$ and $Et_4N[Al_2Cl_7]$. These new compounds were obtained from stoechiometric solutions $R_4NCl:2AlCl_3$ in anhydrous sulphur dioxide (0°C). The sulphur dioxide was evaporated leaving white crystals.

Liquids (*Friedel-Crafts solutions*). The $ArH^+[Al_2X_7]^-$ (Ar = toluene, m-xylene, mesitylene; X = Cl, Br) liquids (molten salts) were obtained at room temperature by

---

*To whom correspondence should be addressed.

bubbling the hydrogen halogenide in a stoechiometric suspension, alkylbenzene: $2AlX_3$. At the end of the reaction all the white, solid AlX_3 disappeared (10–30 h for the chlorides and 3–5 h for the bromides). The alkylbenzenes were previously distilled over P_2O_5 and maintained over molecular sieves.

Spectra

The Raman and i.r. spectra were recorded on a Ph_0 Coderg (He–Ne laser) and a Perkin Elmer 180, respectively. The i.r. spectra were obtained from Nujol mulls between silicium windows. Nujol was previously distilled over sodium and kept over molecular sieves. In the course of the mulls preparation, KAl_2Br_7 suffered a slight non spectroscopically detected decomposition. Owing to their deep orange to red colours the Friedel–Crafts solutions ("red oils") were not Raman recorded. We must underline that the use of three different alkylbenzenes was necessary to facilitate the identification of the $Al_2X_7^-$ and ArH^+ bands in the low frequency range. In fact, the ArH^+ cations give narrow weak bands whose shapes and frequencies appear almost independent of the $Al_2X_7^-$ anions.

RESULTS

Figures 1–3 present the spectra. A strong line (315, 201, 142 cm^{-1}, respectively, for Cl, Br, I*) appears in all the Raman recordings. It is close to the ν_1 line of the corresponding AlX_4^-. Owing to the weak diffusing properties of the tetraalkylammonium salts, this line is the only one recorded in the $Al_2Cl_7^-$ spectra. In the two series AlX_4^- and $Al_2X_7^-$ the Raman spectra of the Cl, Br and I compounds look almost comparable. Quite different is the situation for the absorption spectra,

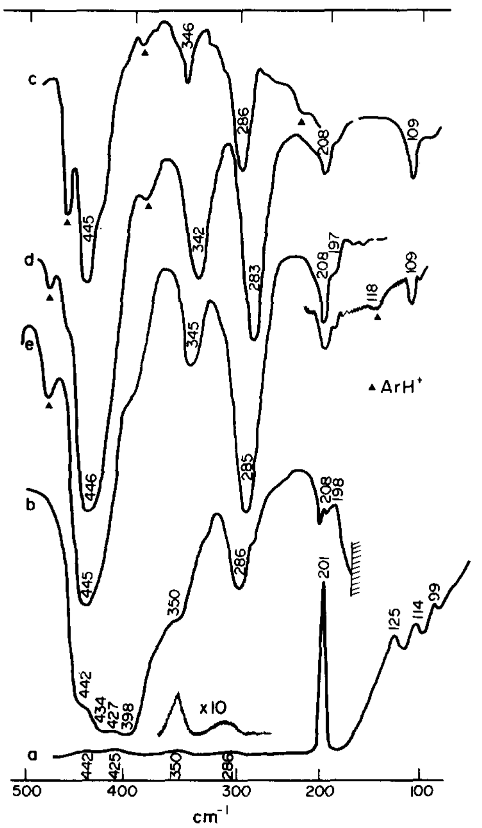

Fig. 2(a–c). Spectra of $Al_2Br_7^-$ anions. (a) Raman spectra of $K^+Al_2Br_7^-$ (cryst.). (b) i.r. spectra of $K^+Al_2Br_7^-$ (cryst.). (c) i.r. 6 Tol $H^+Al_2Br_7^-$ (liq.). (d) i.r. o-Xyl $H^+Al_2Br_7^-$ (liq.). (e) i.r. Mes $H^+Al_2Br_7^-$ (liq.).

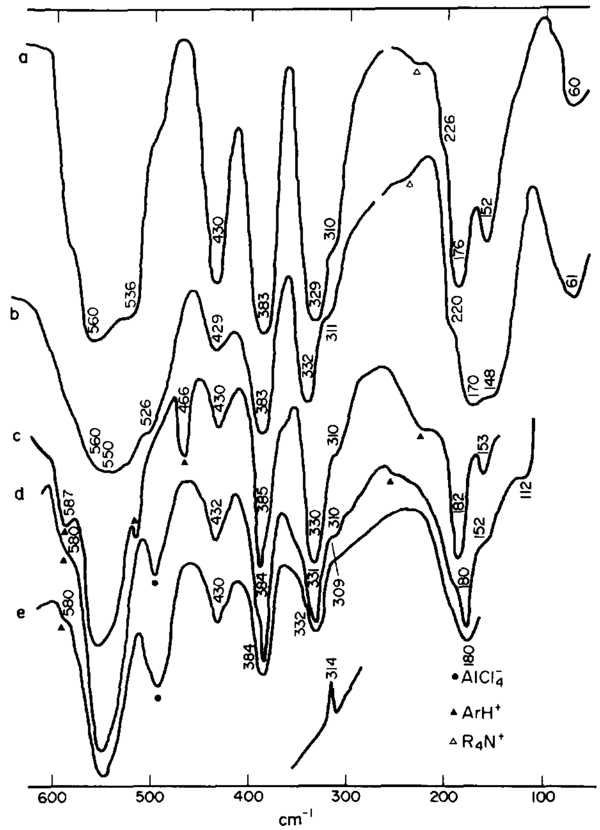

Fig. 1(a–e). Spectra of $Al_2Cl_7^-$ anions. (a) $Et_4N^+Al_2Cl_7^-$ (cryst.) i.r. (b) $Me_4N^+Al_2Cl_7^-$ (cryst.) i.r. (c) $xTolH^+Al_2Cl_7^-$ (liq.) i.r. (d) o–Xyl$^+H^+Al_2Cl_7^-$ (liq.) i.r. (e) Mes $H^+Al_2Cl_7^-$ (liq.) i.r. (f) Raman spectra of $Et_4N^+Al_2Cl_7^-$.

---

*Cl, Br, I are used for $Al_2Cl_7^-$, $Al_2Br_7^-$, $Al_2I_7^-$.

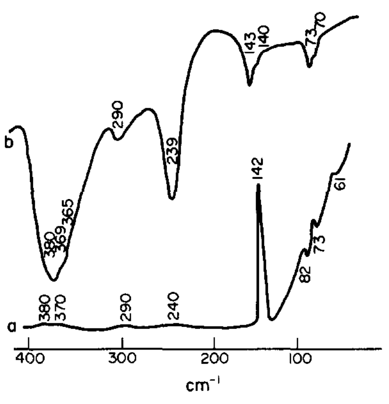

Fig. 3(a–b). Spectra of $Al_2I_7^-$ anions. (a) Raman spectra of $Cs^+Al_2I_7^-$ (cryst.). (b) i.r. spectra of $Cs^+Al_2I_7^-$ (cryst.).

they present principally in the stretching, range clear differencies and the straightforwardness of the AlX_4^- spectra contrasts with the complexity of the wide bands of the $Al_2X_7^-$ spectra. Finally, in the $Al_2X_7^-$ series, the shapes and intensities of the i.r. and Raman recordings look similar, contrasting with the behaviour in the $Ga_2X_7^-$ series, where they highly depend on the halogen.

ASSIGNMENTS AND DISCUSSION

In [1] the vibration analysis was fulfilled in reference to the C_{2v} symmetry and to group vibrations. Here the C_s symmetry is preferred owing to the structure of the KAl_2Br_7 crystal[4]. Actually, $Al_2Br_7^-$ exists also in a C_2 (near C_{2v}) form in $NH_4Al_2Br_7$[5]. However, the general reference to C_s is based not only on the choice of KAl_2Br_7 as reference compound but also on the great number of active i.r. bands in this symmetry and finally on the fact that symmetry bears little effect on the valence force field (see below).

The vibration analysis is made with reference to normal modes and not to valence group modes owing to significant couplings (see below).

In the C_s conformation the $Al_2X_7^-$ ion must give 21 normal modes (13A′ and 8A″), all being i.r. and Raman active. These normal modes appear as mixings of 16 group modes issued from the two X_b–$Al(X_t)_3$ terminal groups (b = bridge, t = terminal), 3 group modes issued from the Al–X_b–Al central bridge group and finally torsions around the bridge bond.

Stretching modes

The 8Al–X stretching modes must occur in the higher frequency range. Among them, 4 terminal asymmetric modes must be essentially related to the Al–X_t bonds. They originate in the splitting of the ν_d vibration of a perturbated, symmetric pyramidal $Al(X_t)_3$ group by the loss of the ternary symmetric and the coupling of the two groups. In the i.r. spectra they look like shoulders on an intense wide band. The corresponding Raman lines are wide and weak. For a given halogen these modes occur in a relatively narrow frequency range but always over ν_3 of the corresponding AlX_4^- ion as shown in Table 2. In this table they are also compared with the modes of some Y–AlX_3 coordination compounds. In all cases they look nearly independent of the Y base and this will be corroborated further by the VFF calculations.

The $\nu_d(AlX_3)$ splitting can be related to the $Te_4^{2+}(Al_2Cl_7^-)_2$[6] and KAl_2Br_7 geometries: the in-the-plan AlX_t bond is shorter by 0.04 Å than the two others, therefore $\nu_a(AlX_3)$ must appear at a lower frequency than $\nu_s'(AlX_3)$. $Al_2I_7^-$ looks dissimilar: to three i.r. frequencies (380, 369 and 365 cm^{-1}) only two Raman frequencies correspond (380, 370 cm^{-1}), therefore a higher *local* symmetry of the AlI_3 group must be considered.

Terminal symmetric stretching modes and bridge stretching modes. The four other stretching modes are related to the $Al(X_t)_3$ terminal symmetric and Al–X_b–Al bridge, stretching motions. They must

Table 2. The four higher stretching modes occur at frequencies higher than $\nu_3(AlX_4^-)$

			ν_s'			ν_a		ν_3
$Al_2Cl_7^-$	Me_4N^+	i.r.	560	550		534	526	
	Et_4N^+	i.r.	560			534	522	
Y–$AlCl_3$	Et_2O	i.r.					525	
	THF	i.r.			540		525	
	Cl^-(Td)							490
$Al_2Br_7^-$	K^+	i.r.	442	434		422	398	
		R	442	430		419	390	
Y–$AlBr_3$	Et_2O	i.r.		438				
	THF	i.r.	457	441				
	Br^-(Td)	i.r R						397
$Al_2I_7^-$	K^+	i.r.	380	369			365	
		R	380	370				
Y–AlI_3	I^-(Td)	i.r.						365

appear in the second frequency range (lower than $\nu_3 AlX_4^-$). In the C_{2v}, $Ga_2Cl_7^-$ case, they were identified as $\nu_s(A_1)$ and $\nu_s(B_1)$ in phase and out of phase couplings of ν_s of the two $GaCl_3$ groups and as $\nu_{sb}(A_1)$ and ν_{ab} (B_1) of the bridge. Here for the anions Cl, Br and I, two i.r. bands and one Raman line appear between ν_1 and $\nu_3(AlX_4^-)$ and two other i.r. bands as well as one Raman line occur near and at lower frequencies than $\nu_1(AlX_4^-)$. It looks *non possible to* assign these bands and lines to *pure motions.*

First take the range under $\nu_1(AlX_4^-)$: two weak bands and a strong line. The strong Raman line is polarized in solutions and so must be assigned to a symmetric mode. The i.r. more intense band, with no corresponding Raman line, must therefore be assigned to an asymmetric mode. As expected it appears at higher frequencies.

The mixing of these two normal modes is disclosed by the behaviour of the Y–AlX_3 spectra for Cl and Br compounds as seen from Table 3.

The ν_s assigned strong Raman line varies with Y and this dependancy proceeds from a strong $\nu_s(AlCl_3) \longleftrightarrow \nu$Al–Y coupling, therefore the strong $Al_2X_7^-$ lines near $\nu_3(AlX_4^-)$ must be assigned to a $\nu_{st} \longleftrightarrow \nu_{sb}$ coupling.

This also explains the proximity between these lines and $\nu_1(AlX_4^-)$. The $\Delta\nu$ value between the strong $Al_2X_7^-$ Raman line and the corresponding $\nu_1(AlX_4^-)$ bears more information. Its decrease (-26, -9, $-3\,cm^{-1}$) from Cl, Br to I must be explained by a stronger and stronger $\nu(AlX_3)$ contribution.

The two last stretching modes occur between ν_1 and $\nu_3(AlX_4^-)$. The lower one (383, 285 and $239\,cm^{-1}$, respectively, for Cl, Br, I) is always strong i.r. and weak Raman. It can be assigned to an asymmetric mode. Conversely the i.r. weak band with its weaker corresponding Raman line (429, 350 and $295\,cm^{-1}$, respectively, for Cl, Br, I) must be a symmetric mode. These two modes can be described as mixings between bridge and terminal vibrations. The bridge part grows with the observed splitting between the two frequencies (46, 65 and $56\,cm^{-1}$, respectively, for Cl, Br, I).

Finally, it must be underlined that for these two modes the symmetric one occurs at lower frequency. This inversion will be explained later (see VFF) by an increase in the interaction between the two bridge bonds.

Deformation modes

Figures 1–3 show that the deformation modes occur at frequencies lower than 225, 150 and $100\,cm^{-1}$, respectively, for Cl, Br, I. Spectra were difficult to obtain in Raman as well as in i.r., especially for solid samples. However, the great number of recordings and the simultaneous use of solutions (organic) and solids (mineral salts) allowed us to obtain correct and reproducible data.

The symmetry analysis leads to 13 deformations and torsion modes but much less are observed (5–6 by spectrum). Indeed, this was also encountered for $Ga_2Cl_7^-$ in [1], where the 10 terminal formations and rotations give only 5 lines or bands, the last observed frequency being assigned to the bridge deformation. As a matter of fact, the terminal groups coupling splittings occurring in this low frequency range are difficult to observe even if they really occur.

The symmetric and asymmetric deformation modes come from $\nu_d(C_{3v})$ of X–AlX_3 by a lowering of the local symmetry. If they could be described in terms of group vibration modes this effect could be interpreted as if X_t–Al–X_t angles were perturbated by the bridge bond. If this perturbation is weak the two modes must be observed in the vicinity of ν_4 for AlX_4^- and of $\nu_d(C_{3v})$ in Y–AlX_3 compounds. This is exemplified in Table 4 in the case of chlorine and bromine compounds.

Two types of assignments can be suggested:

(i) the two i.r. bands and the Raman line can be assigned to δ'_s and δ_a. The missing Raman mode can be assigned to the out of phase δ_a (160, 109 and $70\,cm^{-1}$, respectively, for Cl, Br, I) which is the less symmetric motion. Therefore, 178, 118 and $73\,cm^{-1}$ for Cl, Br, I must be assigned to δ'_s. The order $\delta'_s > \delta_a$ is as expected. The expected angle perturbation appears in the X-ray structure of KAl_2Br_7 [4].

(ii) The low frequency band can be also simultaneously assigned to the in phase δ'_s and δ_a and the higher frequency to the out of phase δ_s.

As we shall see further, the DEP favours the first hypothesis. The δ_s vibrations occur classically over δ'_s and δ_a, therefore, the single Raman active frequencies (126, 82 for Br and I) are assigned to the in phase δ_s.

A comparison between "alkaline" salts and Friedel–Crafts solutions (melts). Though not identified previously but highly suspected from

Table 3. The "ν_s" Raman line varies with the Y ligand

Cl compounds	O–$AlCl_3$	$AlCl_4^-$	$Al_2Cl_7^-$	Br–$AlCl_3$
	388	356	315	308
Br compounds	Cl–$AlBr_3$	O–$AlBr_3$	$AlBr_4^-$	$Al_2Br_7^-$
	247	238	214	201
I compounds			AlI_4^-	$Al_2I_7^-$
			152	142

Table 4. Symmetry and asymmetry deformation modes occurring in the vicinity of $\nu_4(AlX_4^-)$

	$ArH^+[Al_2Cl_7^-]$	$R_4N^+[Al_2Cl_7^-]$	$AlCl_4^-$	$O–AlCl_3$	$Br–AlCl_3$
Cl compounds					
	178	178	180	180	180
	160	152	$\nu_4(Td)$	158	$\nu_d(C_{3v})$
	$ArH^+[Al_2Br_7^-]$	$AlBr_4^-$	$O–AlBr_3$	$Cl–AlBr_3^-$	
Br compounds					
	119	119	125	120	
	109	$\nu_4(Td)$	(C_s)	$\nu_d(C_{3v})$	
		AlI_4^-	$Al_2I_7^-$		
I compounds					
		84	73		
		$\nu_4(Td)$	70		

electrical conductivity and pressure measurements, the $Al_2Cl_7^-$ and $Al_2Br_7^-$ are the unique anions present in the Friedel–Crafts solutions prepared in this work. Moreover no trace of another aluminium compound had been spectroscopically detected. This is an *important chemical new result*, but other consequences are not negligible. Effectively, the similarities in number as well as in frequencies between Friedel–Crafts solutions and solid alkaline salts authorize us to consider the anions in the solid state as isolated species; therefore *site effects and lattice coupling are absent in these salts.*

Significant differencies appear only in the ν_s', ν_a range. There, the wide structured band in solids must be compared with the single narrower and structured band in solutions. Also, the gravity centre is positively shifted (10–25 cm^{-1}) from the solids to the solutions. This behaviour means that the AlX_3 groups in solutions are little perturbated and that their local symmetry is high (near C_{3v}).

VALENCE FORCE FIELD AND DEP OF NORMAL MODES

Basis for the VFF

Valence force field. The normal modes calculations have been carried out by a G.F. method. The IBM 350-60 Schachtsneider program is from FOREL[7]. The force field is of the SHIMANOUCHI[8] localized valence type. It makes use of the local symmetry properties and favours the force constants transferability; therefore it is well adapted to isotopic effect lacking problems.

The internal coordinates and their linear combinations are those used for dimethylether[9]. All diedral angles implied in the torsions have been taken into account. The use of local symmetry coordinates gives DEP's in terms of local group modes.

G matrix. The chosen geometric parameters are given in Table 5. For $Al_2Cl_7^-$ and $Al_2Br_7^-$ they are averages of X-rays structural data. Some observations on the behaviour of the $Al–X_b$ lengths and the $Al–X_b/Al–X_t$ length ratios lead to an estimate of the unknown $Al_2X_7^-$ parameters. Though a previous study has concluded to a linear Ga–I–Ga bridge[10] the lack of selectivity rule effects in the present spectra (as well as in all the $Al_2X_7^-$ series) lead now to an Al–I–Al angular bridge. Lastly, the $X_t–Al–X_t$ and $X_t–Al–X_b$ angles are taken tetrahedral. Therefore, the general chosen $Al_2X_7^-$ symmetry is C_s.

F matrix. The initial force constants are obtained from the X–AlX_3 model. They are transferred from those of the tetrahedral AlX_4^- ions. The $f_\alpha–f_{\alpha\alpha}$ interaction force constant indetermination is removed by the use of the Torkington ellipses method[11]. $F\nu_{sp}$ and $F\nu_{ap}$ are chosen at first in reference to the relative lengths and therefore in reference to the relative bond order ratio b.o. (MCl_b)/b.o. (MCl_t) approximatively equal to 0.5. The normal modes force constants are linear combinations of the internal coordinates force constants (in the C_{3v} point group). For Cl and Br they were first used by FOREL[12] in a study of the

Table 5. Geometric parameters remained in the N.M.C. calculation

		$dAlX_t$	$dAlX_d$	θ(bridge)	Σ covalent radi (Pauling)	$Al_2X_7^-$ $R = (dAlX_b/dAlX_t)$	Symmetry
$Al_2Cl_7^-$	Te_4^{2+}	2.102	2.242	110°	2.24	1.066	C_s
	$Pd_2(C_6H_6)_2^{2+}$	2.100	2.260	115°		1.07	C_{2v}
	*(6a)	2.102	2.242	110°			C_s
$Al_2Br_7^-$	K^+	2.280	2.402	110°	2.39	1.053	C_s
	NH_4^+	2.270	2.430	108°		1.070	C_2
	*	2.280	2.402	110°			
$Al_2I_7^-$	*	2.42	2.58	110°	2.58	1.066	C_s

*Data retained in the normal mode coordinate calculation.

Table 6. Force constants comparison in AlX_4^- and $Al_2X_7^-$ anions

Force constants in terms of symmetry coordinates*	$AlCl_4^-$	$Al_2Cl_7^-$	$AlBr_4^-$	$Al_2Br_7^-$	AlI_4^-	$Al_2I_7^-$
$F\nu_s$	2.44	2.54		2.07	1.507	1.600
			2.25			
$F\nu_a$		2.35		1.92		1.550
	2.11		1.77		1.468	
$F\nu_s'$		2.40		1.97		1.550
$F\delta_s$	0.672	0.672	0.600	0.600	0.629	0.400
$F\delta_d$, Fr_d	0.653	0.653	0.720	0.720	0.525	0.525
$F\nu_{sp}$		1.400		1.400		1.100
$F\nu_{ap}$		1.000		0.900		0.700
$F\theta_p$		0.650		0.660		0.650
$F\tau$		0.200		0.200		0.200
$f(\nu_s - \delta_s)$	0.205	0.205	0.204	0.204		0.250
$f(\nu_s - \nu_{ip})$	+1.89	0.220	0.291	0.100	0.195	0.100
$f(\delta_s - \nu_{ip})$	−0.355	−0.200	−0.355	−0.120	−0.218	−0.100
$f(\nu_d - \delta_d)$	−0.250	−0.250	−0.289	−0.289	−0.190	−0.190
$f(\nu_d - r_d)$	+0.250	+0.250	+0.289	+0.289	+0.130	+0.190
$f(\delta_d - r_d)$	−0.019	−0.019	+0.120	0.120	+0.110	0.110
$f(\Gamma_d - r_d)$		0.100		0.100		0.100
$f(\nu_{sp} - r_p)$		0.200		0.220		0.250
Force constants in terms of internal coordinates						
Fd_{term}		2.44		2.00		1.57
Fd_{bridge}		1.20		1.15		0.90
$R_2 = Fd_{br} : Fe_{term}$		0.50		0.57		0.57
fdd_{bridge}		0.150		0.200		0.200

*mdyn $Å^{-1}$ for bond interactions, mdyn. $Å^{-2}$ rad^{-2} for bridge–bridge interactions, mdyn $Å^{-1}$ rad^{-1} for bridge–bond interactions.

dimethylether–aluminium halogenide complexes. All these constants are given in Table 6.

RESULTS AND DISCUSSION

Stretching modes

The correlation between experimental and calculated frequencies appears suitable from the first calculation cycle. The greatest departure occurs for the normal modes containing a high contribution of bridge bond modes. No noticeable improvement is obtained when F_d diagonal bridge force constant is varied, even over a great range. Therefore, we modified the two interaction force constants $f(\nu_s - \nu_b)$ and $f(\nu_s - \delta_s)$. This was done owing to the fact that these constants are the least transferable ones, since they measure interactions that must be very different from those obtained for the X–AlX_3 groups. Indeed, the correlation was considerably improved. The calculated stretching modes occur in two quite different groups (see assignments). The first four modes appear in the higher frequency range. They can be described as pure ν_{st}' and ν_{at}, respectively, for the A′ mode and the A″ modes. For these four components the observed splitting is weak. This leads us to choose two different values for $F_{\nu' s}$ and $F_{\nu a}$. This way is justified if we recognize that the ν_s' mode depends on the three terminal bonds, whereas ν_a only depends on the two A″ AlX_t bonds and that they are longer than the A′ bond.

In the following frequencies group the symmetric terminal ν_s and the bridge stretchings ν_{sb} and ν_{ab} appear. As seen from the DEP (Table 7) none of these four normal modes can be identified with a single group vibration. This was underlined in the course of the assignment.

In $Al_2Cl_7^-$ the 310 and 336 cm^{-1} bands are essentially ν_{sb} and ν_{ab}, but the 206, 209 cm^{-1} (Br) and 140–143 (I) bands are much more mixed and slightly favour their terminal modes. As seen before this is coroborated by the lowering or the splitting between the two frequencies. The explanation lies in the increase of the halogen weight.

The two higher frequencies (383 and 429 cm^{-1} for Cl) are also highly mixed with about 15% of δ_s. In the lower mode the ν_s and ν_{st} parts are nearly equal but in the higher mode the percent ν_{st} is over the percent ν_{sb} for $Al_2Cl_7^-$ and goes to $st < sb$ for Br and I. Quite logically the major part taken by the bridge bond stretching grows also with the halogen weight.

We have also to elucidate why for these higher modes and in the three anions the ν_s dominated mode is over the ν_a dominated one although for lower modes they behave normally. With this aim several perturbations bearing on geometries and force constants were tested. Among them τ diedral angle variable, which allows to describe the C_{2v}, C_1 and C_s conformations, bears little influence on the stretching modes. On the contrary a variation of the f_{dd} bridge bond–bridge bond interaction force constant gives excellent results (Fig. 4).

Table 7. Comparison between experimental and calculated frequencies of $Al_2X_7^-$ anions

$Al_2Cl_7^-$			$Al_2Br_7^-$			$Al_2I_7^-$		
Frequencies			Frequencies			Frequencies		
Exper.	Calcul.	P.E.D.	Exper.	Calcul.	P.E.D.	Exper.	Calcul.	P.E.D.
560	551		442	436				
		$100\nu'_{ST}AlCl_3$			$100\nu'_{ST}AlBr_3$			
550	540		430	422				
540	535		525	416		380	374	$100\nu'_{ST}AlI_3$
		$100\nu_{aT}AlCl_3$			$100\nu_{aT}AlBr_3$			
526	530		398	410			373	
						370	366	
								$100\nu_{aT}AlI_3$
						365	360	
		$11\delta_s AlCl_3$			$17\delta_s$			$14\delta_s$
429	425	$65\nu_{ST}AlCl_3$	345	342	$32\nu_{ST}$	295	295	$36\nu_{ST}$
		$25\nu_{spont}$			$50\nu_{spont}$			$48\nu_{spont}$
		$18\delta_s AlCl_3$			$18\delta_s$			$17\delta_s$
383	400	$38\nu_{sT}AlCl_3$	299	285	$38\nu_{sT}$	239	254	$40\nu_{sT}$
		$44\nu_{spont}$			$44\nu_{apont}$			$42\nu_{apont}$
		$10\nu_{ST}$			$11\delta_s$			$47\nu_{sT}$
336	332		207	209	$54\nu_{sT}$	143	143	$35\nu_{apont}$
		$85\nu_{apont}$			$25\nu_{apont}$			
		$12\nu_{sT}$			$12\delta_s$			$59\nu_{sT}$
310	316		198	206	$59\nu_{sT}$	140	140	
		$75\nu_{spont}$			$20\nu_{apont}$			$26\nu_{sp}$
		$39\delta s$			$42\delta_s$			
226	218	$24\ r\|$		139				
		$20\delta_{spont}$			$39\ r_{\parallel}$			
		$84\delta_s$			$68\delta_s$			$52\delta_s$
—	196		125	125			84	
		$11\ r_{\parallel}$			$29\ r_{\parallel}$			$33\ r_{\parallel}$
								$68\delta_s$
						82	80	
								$29\ r_{\parallel}$
		$60\delta_a$		110				
176	175		114		$100\delta'_s$			
		$40\ r$		110				
	171	$82\delta_a$		109		73	70	$100\delta'_s$
					$100\delta_a$			
		$40\ r$		107		70	70	$100\delta_a$
	171	$90\delta'_s$						
152	169	$85\delta'_s$		103				
			99		$100\ r$			
				80	$90\ r$	61	60	$100\ r$
		$73\ r$						
	162		72	78	$20\delta_s$, $67\ r_{\parallel}$			
		$26\delta'_a$						
		$80\ r$						$22\delta_s$
	110		67	70	$29\delta_s$, $61\ r_{\parallel}$		53	$64\ r_{\parallel}$
		$16\delta'_a$				50		
112							52	$88\ r$
		$37\ r_{\parallel}$						
	110	$28\delta_s$	—	35	$70\delta_p$, $20\ r_{\parallel}$			
		$14\delta'_s$						
	110	$77\ r_{\parallel}$	—	28	100τ	42	44	$56\delta_s$
				20				$28\ r_{\parallel}$
		$13\delta'_s$				—	24	$100\delta_p$
	54	$70\delta_p$						
		$18\ r_{\parallel}$						
—	48					—	14	

*Pont = bridge = *b*.

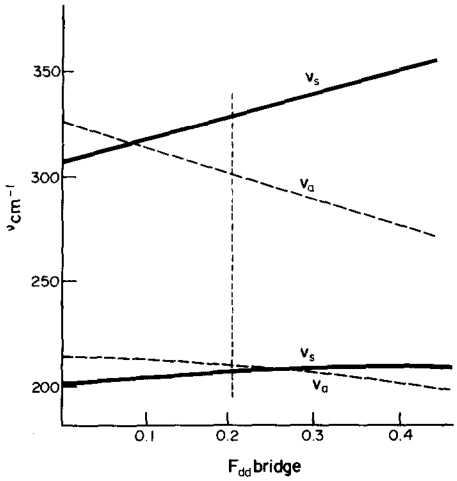

Fig. 4. Bridged stretching modes Al–Br versus the bridge force constant interaction F_{dd} in $Al_2Br_7^-$.

Deformations modes

In the deformation range the VFF calculation gives three distinct subranges whatever is the considered halogen. A first group of two modes is δ_s symmetric deformation and $r\|$ rotation dominated. In the C_{3v} model the two group modes belong to different species, therefore they are not coupled. However, the symmetry lowering in $Al_2X_7^-(C_s)$ allows the coupling; they become A′ and can be essentially observed in the Raman spectra. The second group gathers four modes. They are dominated by the δ_s' and δ_a group deformation modes and therefore can be observed in i.r. as well as in Raman.

Finally, in the last group the dominating group modes are $r\|$ and $\perp$. The initial force field gives an important splitting that can be reduced by the introduction of a perpendicular torsion–rotation interaction constant. The diagonal and interaction force constants related to the deformation and rotation modes are identical to the initially introduced ones. They are directly transferable. From the first calculation cycle they lead to a suitable agreement between experience and theory. This agreement can be improved by a differentiation between, for example, the F_{rr} and F_{rd} but this gives no improvement on the quality of the force field.

Finally, the $f_{\theta b}$ bridge deformation constant has been estimated by the empirical formula $f_{\theta p} = d^2F_d/10$. This leads to $\delta_p \simeq 54\,\mathrm{cm}^{-1}$ for $Al_2Cl_7^-$. This is to be challenged with a wide band observed at $58\,\mathrm{cm}^{-1}$. As a consequence, the δ_p for $Al_2Br_7^-$ are respectively expected near 33 and $24\,\mathrm{cm}^{-1}$. The torsional modes τ expected at lower frequencies are not observed.

A comment about force constants and frequencies

The essential result is a good transferability of the initial force constants. This leads to general VFF for the three anions. Practically all the experimental facts are explained by this initial choice of force constants and geometries (GF matrix).

The modified force constants are $f(\nu_s - \nu_b)$ and $f(\nu_s - \delta_s)$ the differentiated $F_{\nu'_s}$ and F_{ν_a} (issued from F_{ν_d}), and the f_{dd} bridge interaction.

Also noteworthy is the ratio (F_{br}/F_{term}) and looks as measurement of the relative strengths of the bridge and terminal Al–X bonds (0.50, 0.57 and 0.57, respectively, for Cl, Br, I).

REFERENCES

[1] A. MANTEGHETTI, D. MASCHERPA-CORRAL and A. POTIER, *Spectrochim. Acta*, **37A**, 211 (1981). (a) A. KINSELLA and J. CORWARD, *Spectrochim. Acta* **26A**, 344 (1970); (b) G. TORSI, G. MAMANTOV and G. M. GEGUN, *Inorg. Nuclear. Chem. Letters*. **6**, 553 (1970); (c) G. M. BEGUN, C. R. BOSTON, G. TORSI and G. MAMANTOV, *Inorg. Chem.* **10**, 886 (1971). (d) H. A. OZY and J. RITTER, *J. Inorg. Nuclear. Chem.* **35**, 1185 (1973). (e) N. R. SNYRL, G. MAMANTOV and L. MCCURRY, *J. Inorg. Nucl. Chem.* **40**, 1489 (1978). (f) R. J. GAK and R. A. OSTERYOUG, *Inorg. Chem.* **19**, 2240 (1980). (g) R. J. GAK, B. GILBERT and R. A. OSTERYOUG, *Inorg. Chem.* **17**, 2728 (1978).

[2] S. M. ARKHIPOV, V. I. MIKHEEVA and T. V. REVZINA, *Russ. J. Inorg.* **13**, 1013 (1968).

[3] See for example, PERKHAMPUS, E. BAUMGARTEN, Proton additions complexes of aromatic hydrocarbons, *Angew. Chem. Int. Ed.* **3**, 12 (1974).

[4] E. RYTTER, B. E. D. RYTTER, H. A. OYE and J. KROGH-MOE, *Acta Cryst.* **B29**, 1541 (1973).

[5] E. RYTTER, B. E. D. RYTTER, H. A. OYE and J. KROGH-MOE, *Acta Cryst.* **B31**, 2177 (1975).

[6] J. D. CORBETT, T. W. COUCH and D. A. COKKENS, *J. Inorg. Chem.* **11**, 357 (1972).

[7] J. H. SCHATSCHNEIDER and R. G. SNYDER, *Spectrochim. Acta.* **19**, 117 (1963).

[8] T. SCHIMANOUCHI, The molecular force field, Physical Chemistry Vol. IV, 287–293.

[9] J. LABARBE, M. T. FOREL and B. BOSSIS, *Spectrochim. Acta.* **24**, 2165 (1968).

[10] D. MASCHERPA and A. POTIER, *Inorganic and nuclear Chemistry* **38**, 211, (1976).

[11] P. TORKINGTON, *J. Chem. Phys.* **17**, 357 (1949).

[12] J. DEROUAULT and M. T. FOREL, *Inorg. Chem.* **16**, 3207 (1977).